Supplementary Materials for

Exfoliation of a Metal-Organic Framework Enabled by Post-Synthetic Cleavage of a Dipyridyl Dianthracene Ligand

*Madison E. Logelin, Eric Schreiber, Brandon Q. Mercado, Michael J. Burke, Caitlin M. Davis, Amymarie K. Bartholomew**

The Department of Chemistry, Yale University, P. O. Box 208107, New Haven, Connecticut, 06520, USA.
E-mail: amymarie.bartholomew@yale.edu

Table of Contents

A. Materials and Instrumentation

Materials

All reactions were performed open to atmosphere, unless otherwise noted. All commercial reagents and solvents were used as provided. All final products were dried in vacuo prior to reporting yields.

Instrumentation

Nuclear Magnetic Resonance (NMR) Spectroscopy: ^{1}H NMR data were recorded on an Agilent DD2 400 MHz spectrometer. ^{13}C NMR data were recorded on an Agilent DD2 600 MHz spectrometer. All resonances in the ^{1}H and 13C NMR spectra are referenced to residual proteo chloroform ($CHCl_3$, δ 7.26 ppm) or dimethyl sulfoxide (DMSO, δ 2.50 ppm). Resonances were singlets unless otherwise noted.

Thermogravimetric Analysis (TGA): TGA was performed on a TA Instruments TGA550 analyzer under a N_2 atmosphere. 2-5 mg of sample was loaded onto a tared Pt pan for analysis and the temperature was ramped from 25 °C to 650 °C at a rate of 10 °C/min.

Differential Scanning Calorimetry (DSC): DSC measurements were performed on a TA Instruments DSC250 instrument. 2-5 mg of sample was loaded in a TA Instruments Tzero Pan and sealed with a Tzero Lid using a press. Temperature was initially cooled to and held at –10 °C for 5 minutes, then ramped from –10 °C to 300 °C at a rate of 5 °C/min.

Solid State UV-vis (SS UV-vis) Spectroscopy: SS UV-vis spectra were recorded on a Shimadzu 3600 Plus Spectrophotometer with an ISR-603 integrating sphere with a $BaSO_4$ reference. Data was collected in diffuse reflectance mode and then inverted and normalized as a representation of absorbance.

Attenuated Total Reflectance Fourier Infrared (ATR-FTIR) Spectroscopy: FTIR spectra were collected using a Thermo Fisher Scientific Nicolet iS5 spectrometer with an iD5 ATR accessory.

Optical Photothermal Infrared (O-PTIR) Spectroscopy: Infrared spectra using O-PTIR were collected on a mIRage-LS IR microscope (Photothermal Spectroscopy Corporation, Santa Barbara, CA) with a four-module-pulsed quantum cascade laser (QCL) system (Daylight Solutions, San Diego, CA). Spectra were collected from 932 cm-1 to 1816 cm-1 in standard (reflective) mode using an average of 10 scans. Collection was performed using a 40X Cassegrain objective. All data was collected on crystalline samples mounted on freshly plasma etched Si/SiO2 wafers.

Plasma Etching Silicon Wafers: Plasma etching of thermal oxide coated silicon wafers was performed by subjecting wafers to O_2 plasma for at least two minutes in a Plasma Etch, Inc. PE-25-LF etcher using ambient air as the O_2 source.

Scanning Electron Microscopy (SEM): SEM imaging was performed on a Hitachi SU8230 UHR Cold Field Emission (CFE) SEM. Samples of pristine **1** and bulk annealed **2** were drop cast from a hexane suspension onto 300 nm thermal oxide coated silicon wafers that had been plasma etched

for five minutes and allowed to air dry. Crystals of **2** were exfoliated onto 300 nm thermal oxide coated silicon wafers that had been plasma etched for five minutes. Samples were sputter coated with Iridium (7 nm) using a Leica ACE600 High Vacuum Sputter prior to analysis due to the insulating nature of the MOF.

X-Ray Photoelectron Spectroscopy (XPS): XPS was collected on a PHI VersaProbe III AD Scanning XPS Microprobe. Samples of pristine **1** and bulk annealed **2** were drop cast from a hexane suspension onto 300 nm thermal oxide coated silicon wafers that had been plasma etched for five minutes and allowed to air dry. Crystals of **2** were exfoliated onto 300 nm thermal oxide coated silicon wafers that had been plasma etched for five minutes.

Atomic Force Microscopy (AFM): AFM images were collected using a Bruker Dimension Fastscan AFM in peak force mode. Samples were prepared by exfoliating annealed MOF crystals onto 300 nm thermal oxide coated silicon wafers. Images were processed in Gwyddion.

X-Ray Diffraction (XRD): Low-temperature diffraction data (ω-scans) were collected on a Rigaku MicroMax-007HF diffractometer coupled to a Saturn994+ CCD detector with Cu Kα (λ = 1.54178 Å). The diffraction images were processed and scaled using Rigaku Oxford Diffraction software (CrysAlisPro; Rigaku OD: The Woodlands, TX, 2015). Using Olex2,[1] the structure was solved with the SHELXT[2] structure solution programing using Intrinsic Phasing and refined against F^2 on all data by full-matrix least squares with SHELXL.[3] All non-hydrogen atoms were refined anisotropically. Hydrogen atoms were included in the model at geometrically calculated positions and refined using a riding model. The isotropic displacement parameters of all hydrogen atoms were fixed to 1.2 times the U value of the atoms to which they are linked. The full numbering scheme of the compound **1** can be found in the full details of the X-ray structure determination (CIF), which is included as Supporting Information. The structure of **1** has been deposited with the CCDC, with deposition number 2342280. These data can be obtained free of charge from The Cambridge Crystallographic Data Center via http://www.ccdc.cam.ac.uk/conts/retrieving.html

Microcrystal Electron Diffraction (MicroED): Data were collected on an XtaLAB Synergy-ED electron diffractometer. The crystals were kept at 100.00 K during data collection. The diffraction from three grains were integrated and merged to produce the reflection list. Using Olex2,[1] the structure was solved with the SHELXT[2] structure solution program using Intrinsic Phasing and refined with the SHELXL[3] refinement package using Least Squares minimization. To achieve a stable refinement, all thermal parameters were restrained to be similar to one another with a standard uncertainty of 0.002. Hydrogen atoms were included in the model at geometrically calculated positions and refined using a riding model. The low data to parameter ration and weak diffraction contributed to the non-ideal least squares refinement. The isotropic displacement parameters of all hydrogen atoms were fixed to 1.2 times the U value of the atoms to which they are linked. The full numbering scheme of the compound **2** can be found in the full details of the X-ray structure determination (CIF), which is included as Supporting Information. The structure of **2** has been deposited with the CCDC, with deposition number 2356228. These data can be obtained free of charge from The Cambridge Crystallographic Data Center via http://www.ccdc.cam.ac.uk/conts/retrieving.html

B. Synthetic Procedures

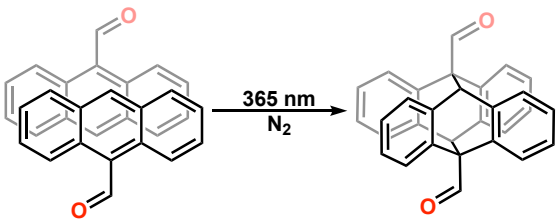

diAn^{CHO}. Although 9,9'-dianthraldehyde has been reported in literature,[4-7] this dimer was synthesized by modifying a dimerization procedure for 9-anthracenecarboxylic acid.[8] 9-anthraldehyde (40 g) was added to a 150 mL Pyrex Erlenmeyer flask containing 100 mL tetrahydrofuran (THF) to form a saturated solution. The solution was sparged under N_2 for 40 min then irradiated under a 365 nm light. After 60 h, a beige precipitate formed which was filtered and washed with THF (2 x 25 mL). The filtrate was recovered, reconcentrated, and recycled for future syntheses.
Yield: 1.78 g, 4.4%
^{1}H NMR (400 MHz, DMSO-d_6) δ 10.15 (s, 2H), 7.00 – 6.94 (d, 4H), 6.93 – 6.82 (m, 6H), 6.7 – 6.59 (d, 4H), 6.93 – 6.82 (s, 2H).

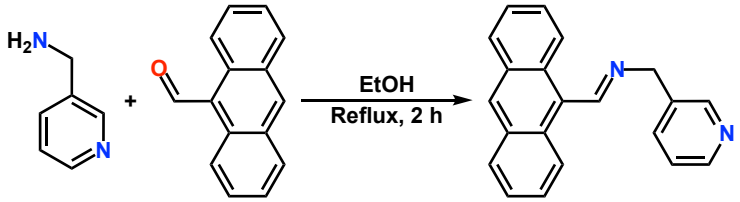

An$^{CNC-3Py}$. The monomer ligand was synthesized according to a literature procedure.[9]

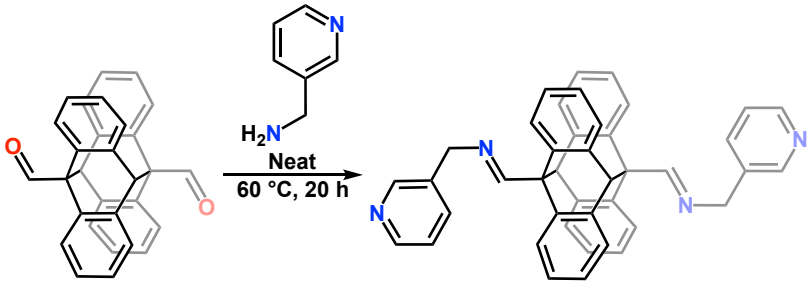

diAn$^{CNC-3Py}$. In a 20 mL vial, **diAn^{COH}** (250 mg) was added to neat 3-picolylamine (4 mL). The reaction was left stirring for 20 h in a 60 °C sand bath. The white precipitate was filtered and washed with methanol (MeOH) and hexane, then dried under vacuum.
Yield: 339 mg, 94.4%
^{1}H NMR (400 MHz, $CDCl_3$) δ 8.91 – 8.85 (s, 2H), 8.69 – 8.61 (d, 2H), 8.37 – 8.32 (s, 2H), 7.96 – 7.91 (d, 2H), 7.47 – 7.42 (dd, 2H), 6.99 – 6.94 (d, 4H), 6.86 – 6.76 (m, 8H), 6.67 – 6.62 (d, 2H), 6.10 – 6.06 (s, 2H), 5.18 – 5.15 (s, 4H).
^{13}C NMR (600 MHz, $CDCl_3$) δ 168.20, 149.34, 148.81, 144.07, 143.80, 135.45, 135.31, 128.67, 126.32, 125.47, 125.37, 123.81, 61.93, 61.03, 51.90.
High-res ESI FTMS (THF) *m/z*: $[M+H]^+$ for $C_{21}H_{16}N_2$ +H; calculated 297.1386; found, 297.1370; 0.0016 ppm error.

$Zn_3(BDC)_3(Py)_2$. The 2D MOF was synthesized by modifying a previous procedure.[10] A 1:1:4 mixture of $Zn(NO_3)_2 \cdot 6H_2O$: 1,4-benzenedicarboxylic acid (BDC): pyridine in DMF was sonicated for 30 s, then put into an 85 °C oven. After 72 h, colorless rod-shaped crystals formed. The crystals were washed with DMF.

$Zn_3(BDC)_3(diAn^{CNC\text{-}3Py})$ (1). $Zn(NO_3)_2 \cdot 6H_2O$ (50.2 mg, 0.169 mmol, 1 eq) was dissolved in 0.5 mL N, N-dimethyl formamide (DMF) then added to a suspension of $diAn^{CNC\text{-}3Py}$ (100 mg, 0.169 mmol, 1 eq) and 1,4-benzenedicarboxylic acid (BDC) (112 mg, 0.675 mmol, 4 eq) in 3.5 mL DMF. The solution was sonicated for 30 s, then put into an 85 °C oven. After 72 h, colorless, plate-shaped crystals formed and the DMF was decanted while the crystals were washed with DMF, THF, and hexane.
Yield: 60.8 mg, 74.9%

$Zn_3(BDC)_3(An^{CNC\text{-}3Py})_2$ (2). Crystals of **1** were left to dry at room temperature overnight. Crystals were then put into a 160 °C oven for 18 h.

Exfoliation of 2. Crystals of **2** were mechanically exfoliated using Scotch Magic™ tape. The exfoliation on Magic tape was carried out under ambient conditions. Single crystals of **2** were tessellated onto Magic tape and then cleaved along the stacking axis two to four times before being transferred onto Si/SiO_2 substrates that had been subjected to O_2 plasma for two minutes. The exfoliated flakes were transferred onto the Si/SiO_2 substrates by heating the substrates with the Magic tape adhered to them at 100 °C for two minutes, cooling for five minutes, and then quickly peeling off the Magic tape.

Exfoliation of $Zn_3(BDC)_3(Py)_2$. The same procedure as the exfoliation of **2** was used.

Digestion of 2. Crystals of **2** were added to MeOH and sonicated for 30 s to form a suspension. Monitoring by pH paper, drops of ~0.9 M sulfuric acid (H_2SO_4) were added until the solution was acidic. The clear, orange solution was stirred for 30 s, then neutralized with triethylamine. The solution was filtered and dried under high vacuum for 2 h.

C. Ligand Characterization

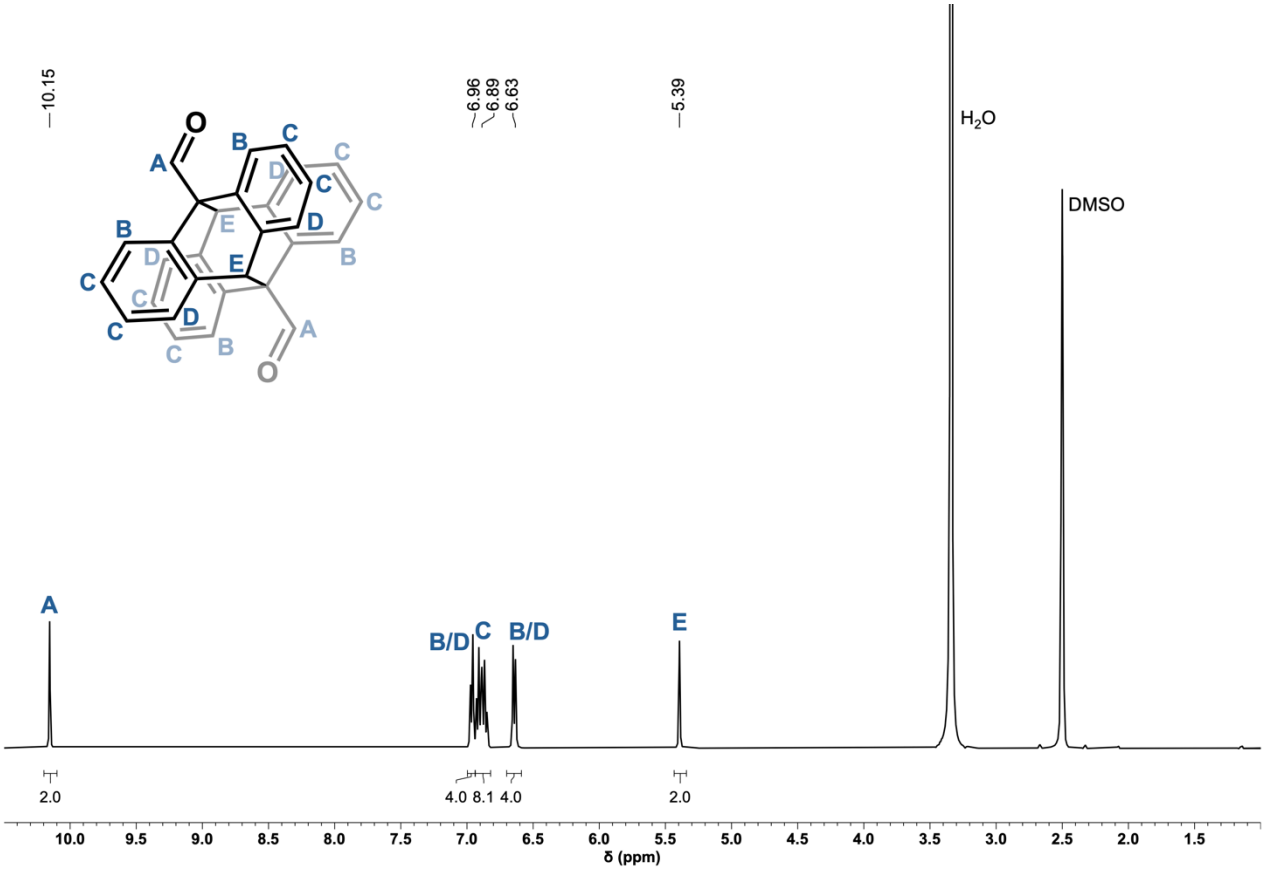

Figure S1. ^{1}H NMR spectrum (400 MHz, DMSO-d_6) of **diAn^{CHO}**.

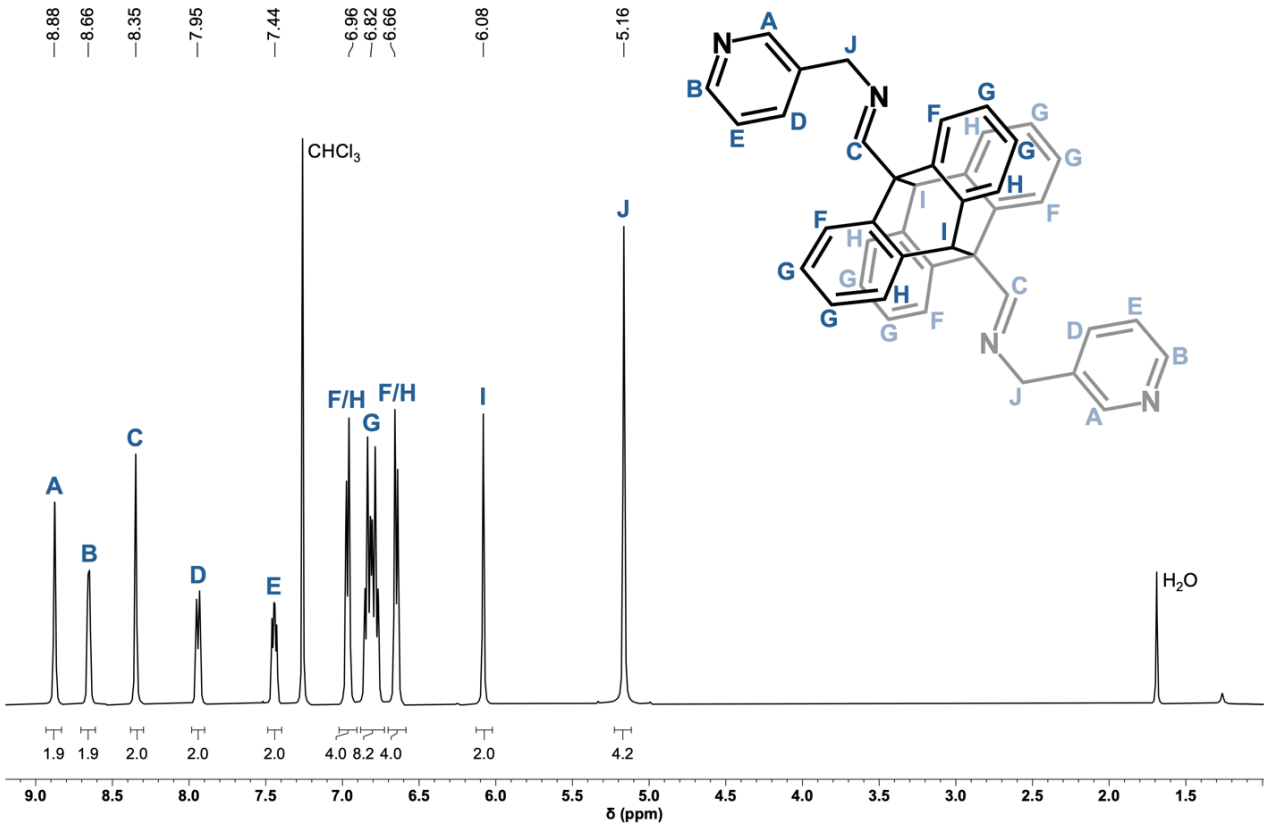

Figure S2. ^{1}H NMR spectrum (400 MHz, $CDCl_3$) of **diAn$^{CNC\text{-}3Py}$**.

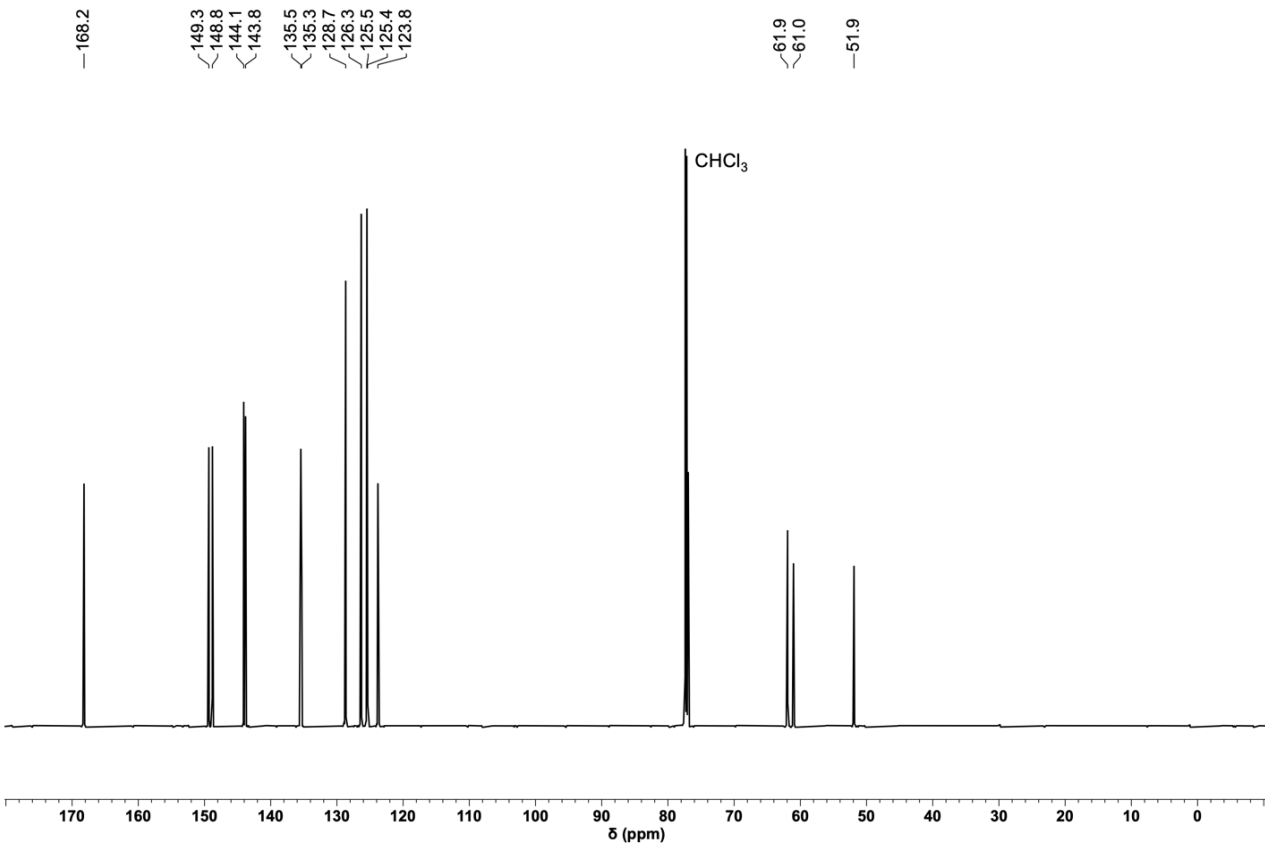

Figure S3. ^{13}C NMR spectrum (600MHz, $CDCl_3$) of **diAn$^{CNC\text{-}3Py}$**.

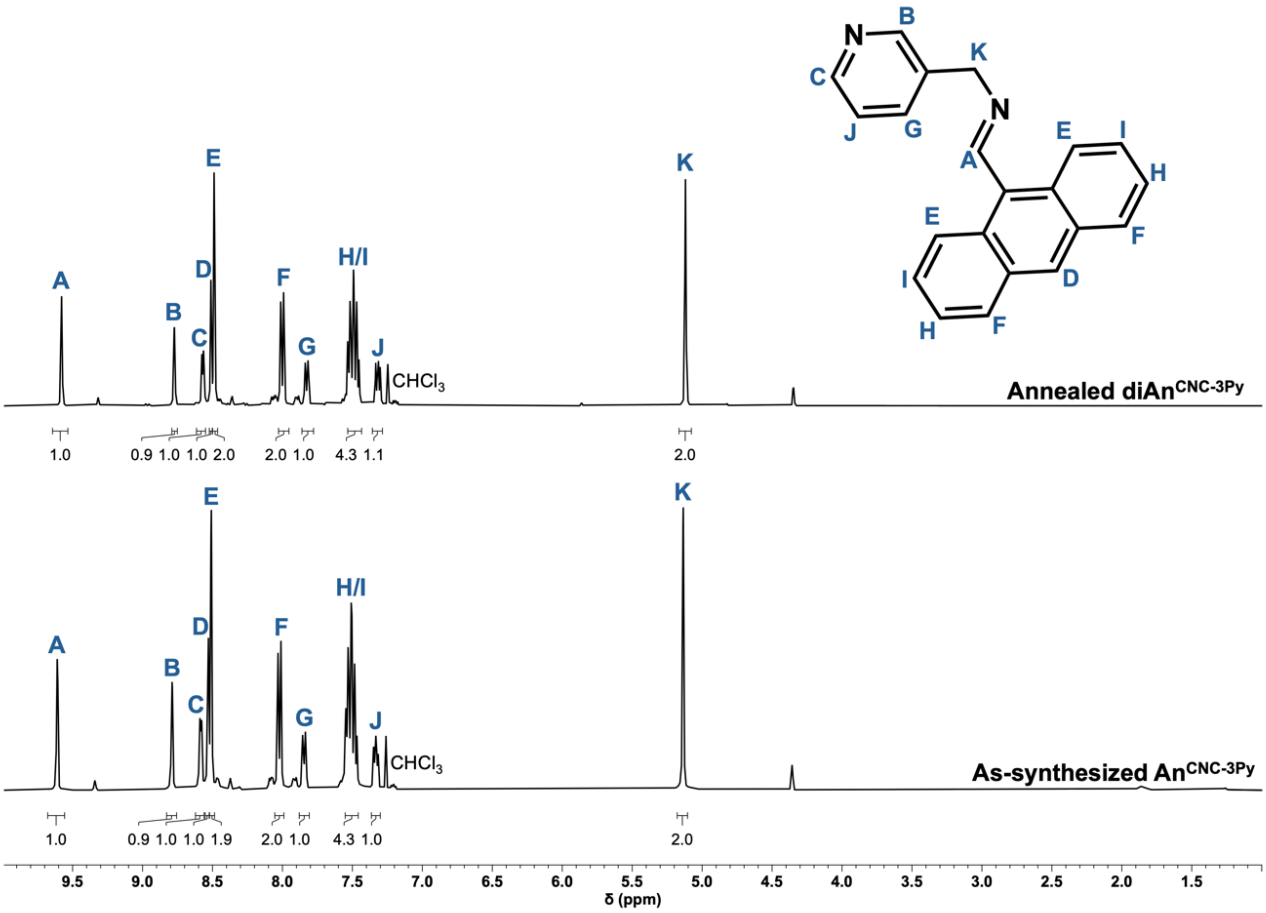

Figure S4. ^{1}H NMR spectra (400MHz, $CDCl_3$) of **diAn$^{CNC\text{-}3Py}$** annealed at 196 °C for 10 minutes (top) and as-synthesized **An$^{CNC\text{-}3Py}$** (bottom).

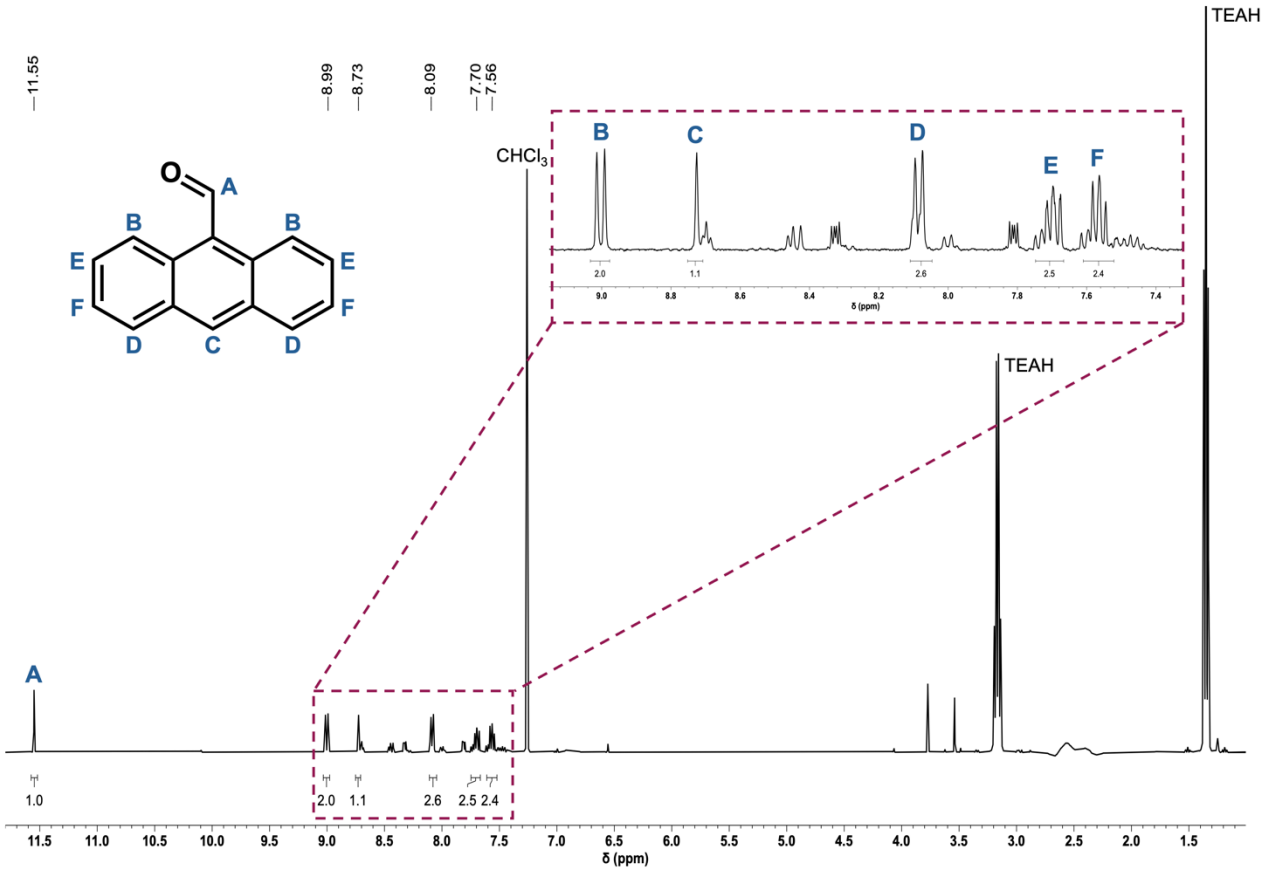

Figure S5. ^{1}H NMR spectrum (400MHz, $CDCl_3$) of **2** after digestion with H_2SO_4. The two strongest peaks are attributed to triethylammonium (TEAH). Strong acids hydrolyze the imine bond in **An$^{CNC\text{-}3Py}$** to produce 3-picolylamine and 9-anthraldehyde. While drying the sample under high vacuum, the 3-picolylamine (b.p. 73-74 °C/ 1mmHg[11]) presumably evaporated, however, the spectrum contains peaks attributed to 9-anthraldehyde.

D. Thermogravimetric Analysis

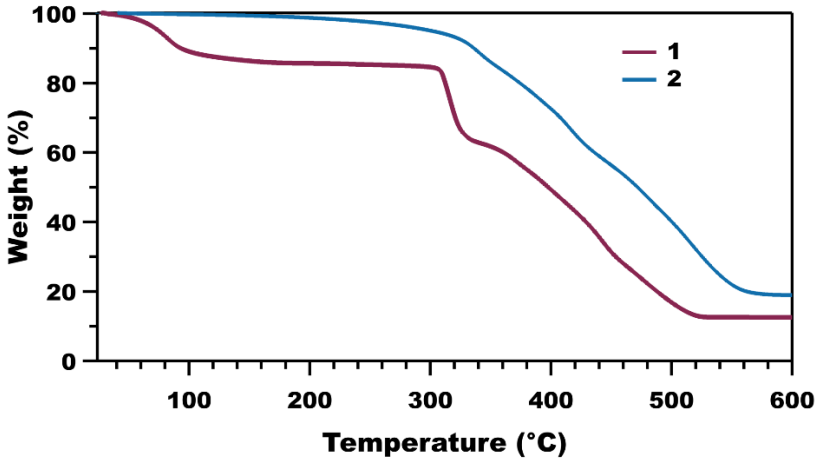

Figure S6. TGA of **1** and **2**.

E. Differential Scanning Calorimetry

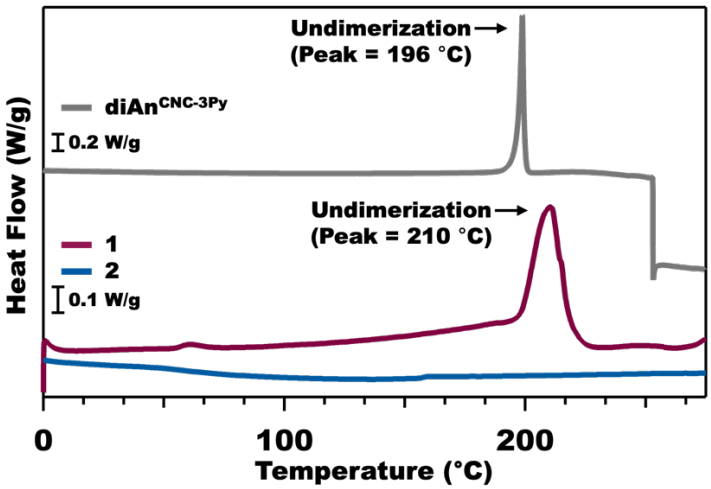

Figure S7. Full DSC of **diAn**$^{\text{CNC-3Py}}$, **1** and **2**. Temperature was initially cooled to and held at –10 °C for 5 minutes, then ramped from –10 °C to 300 °C at a rate of 5 °C/min. The ligand, **diAn**$^{\text{CNC-3Py}}$, starts to melt at 250 °C.

F. Infrared Spectroscopy

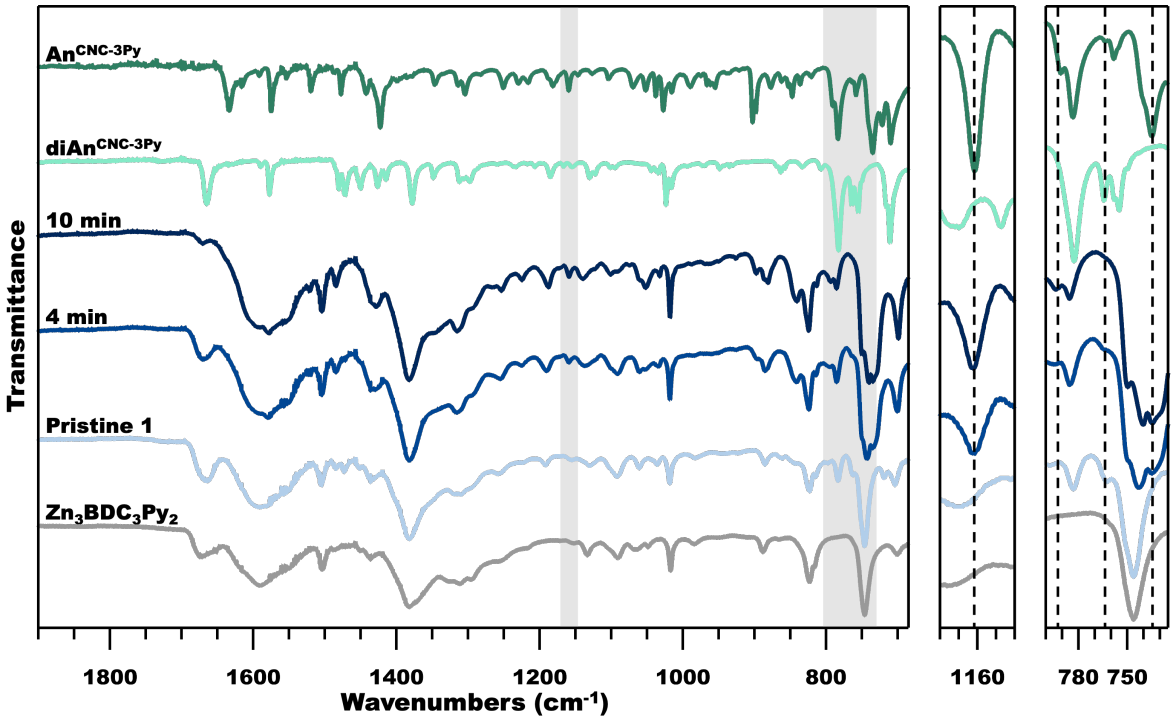

Figure S8. Full normalized ATR-FTIR spectra of the undimerized ligand, **An**$^{\text{CNC-3Py}}$, **diAn**$^{\text{CNC-3Py}}$, pristine MOF **1**, annealed MOF **1** at 210 °C, and 2D MOF $Zn_3BDC_3Py_2$. Tracking the annealing process through ATR-FTIR spectroscopy indicates that the 2D Zn_3BDC_3 sheets remain intact. The ATR-FTIR spectrum of the known pyridine-capped **2** analogue, $Zn_3BDC_3Py_2$,[6] which has an identical structure in the 2D plane to **1**, strikingly resembles the components of the IR spectra of **1** that remain unchanged upon annealing to **2**. Additionally, the peaks associated with the undimerization of anthracene can be distinguished through comparison with An$^{\text{CNC-3Py}}$, the ligand monomer, and diAn$^{\text{CNC-3Py}}$. This analysis holds for the full spectrum, but it is useful to discuss a few regions in detail as an illustration. At 1159 cm^{-1}, 792 cm^{-1}, and 735 cm^{-1}, peaks consistent with the ligand monomer can be seen growing in, whereas the shoulder at 764 cm^{-1}, consistent with the ligand dimer, diminishes as **1** is annealed.

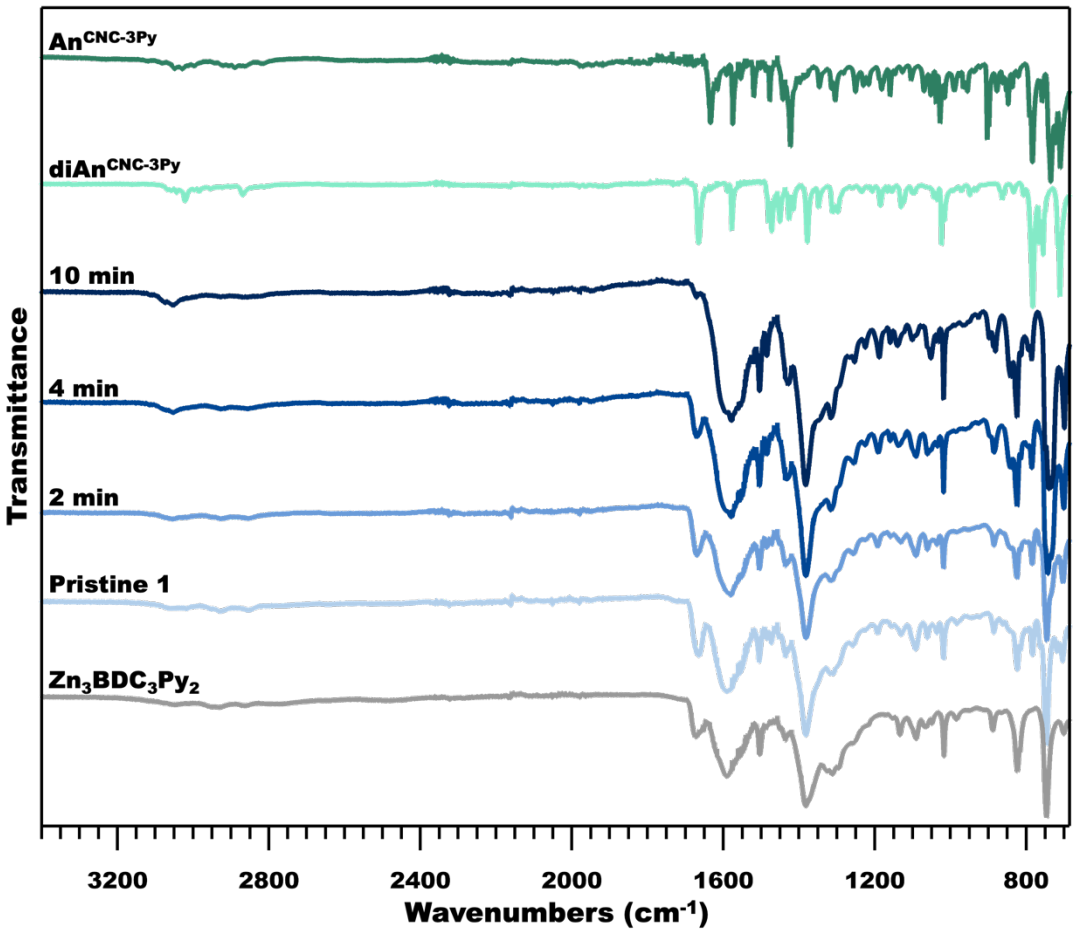

Figure S9. Full normalized ATR-FTIR spectra of the undimerized ligand, **An**$^{CNC\text{-}3Py}$, **diAn**$^{CNC\text{-}3Py}$, pristine MOF **1**, annealed MOF **1** at 210 °C, and 2D MOF $Zn_3BDC_3Py_2$. DMF peaks are included in the MOF spectra at 2940 cm^{-1}, 2852 cm^{-1}, 1687 cm^{-1},1502 cm^{-1},1403 cm^{-1}, 1384 cm^{-1}, 1260 cm^{-1}, 1086 cm^{-1}, and 859 cm^{-1}.[12]

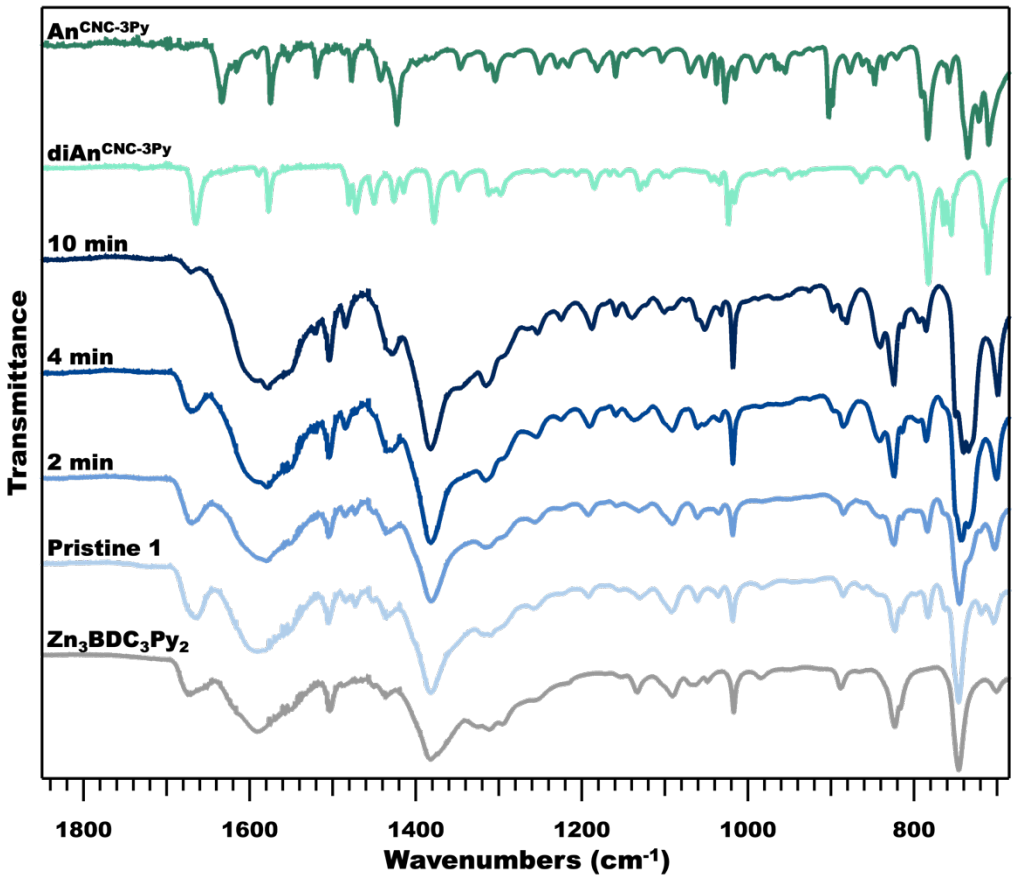

Figure S10. Normalized ATR-FTIR spectra of the undimerized ligand, **An**$^{CNC-3Py}$, **diAn**$^{CNC-3Py}$, pristine MOF **1**, annealed MOF **1** at 210 °C, and 2D MOF $Zn_3BDC_3Py_2$. DMF peaks are included in the MOF spectra at 1687 cm^{-1},1502 cm^{-1},1403 cm^{-1}, 1384 cm^{-1}, 1260 cm^{-1}, 1086 cm^{-1}, and 859 cm^{-1}.[12]

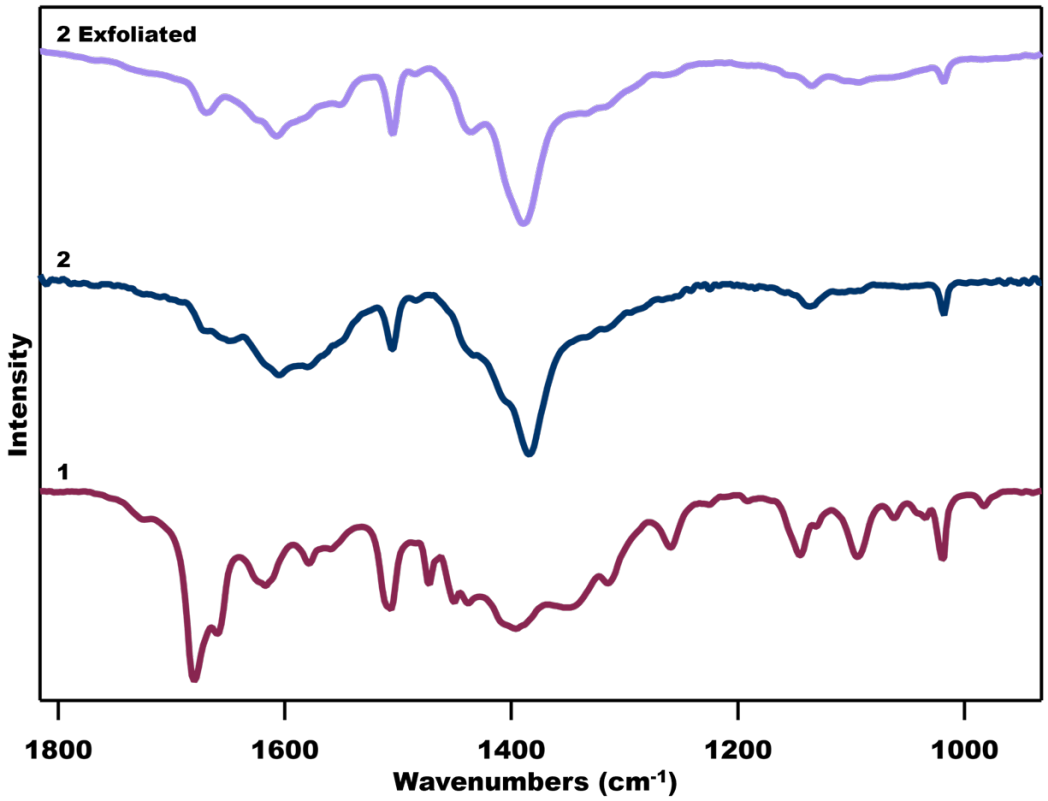

Figure S11. Normalized and averaged O-PTIR spectra of **1**, **2**, and exfoliated MOF **2**. Spectra of exfoliated samples of **2** are plotted as averages of normalized data collected in triplicate on each of three crystals. All other spectra are reported as normalized averages of a total of nine spectra collected across three unique crystals.

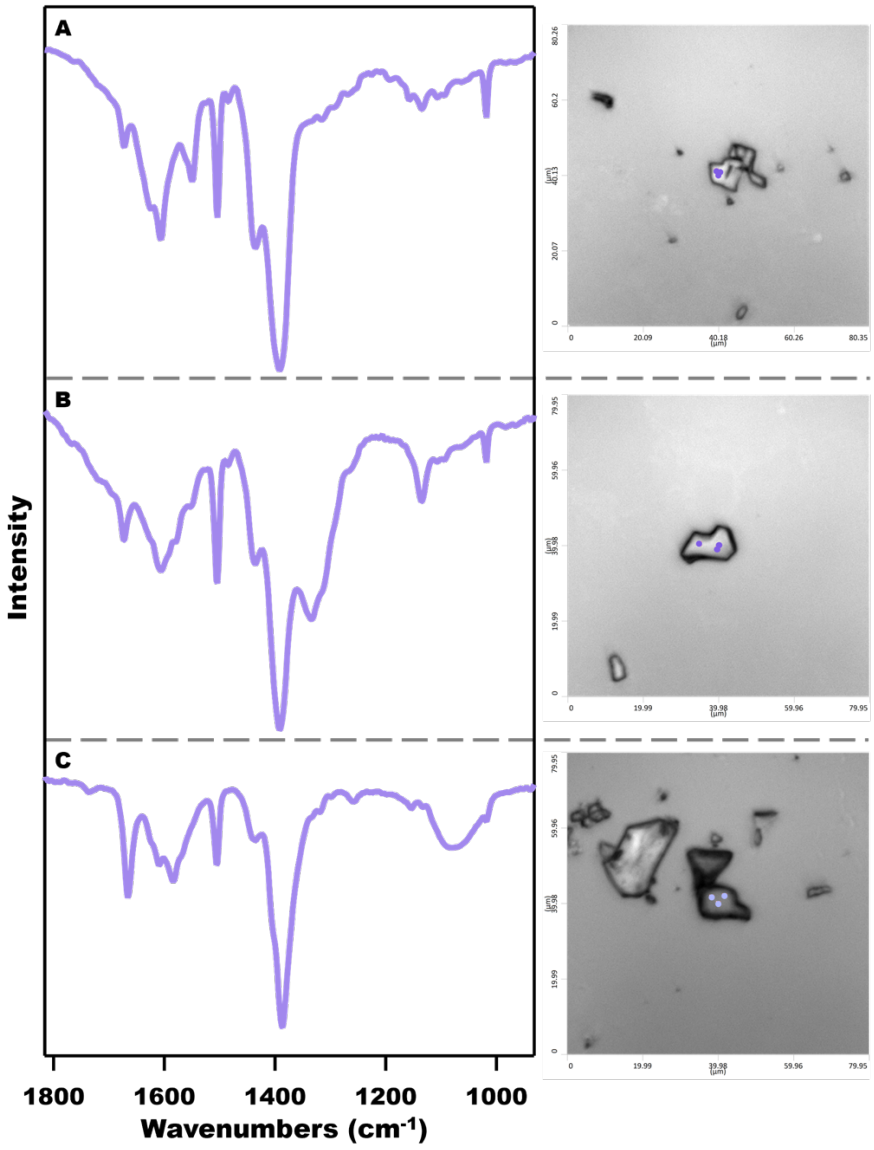

Figure S12. Normalized and averaged O-PTIR spectra of exfoliated MOF **2** (left) with optical images of each sample (right). Each spectrum is an average from 3 unique spots on the flake, which are shown as purple dots.

G. Scanning Electron Microscopy

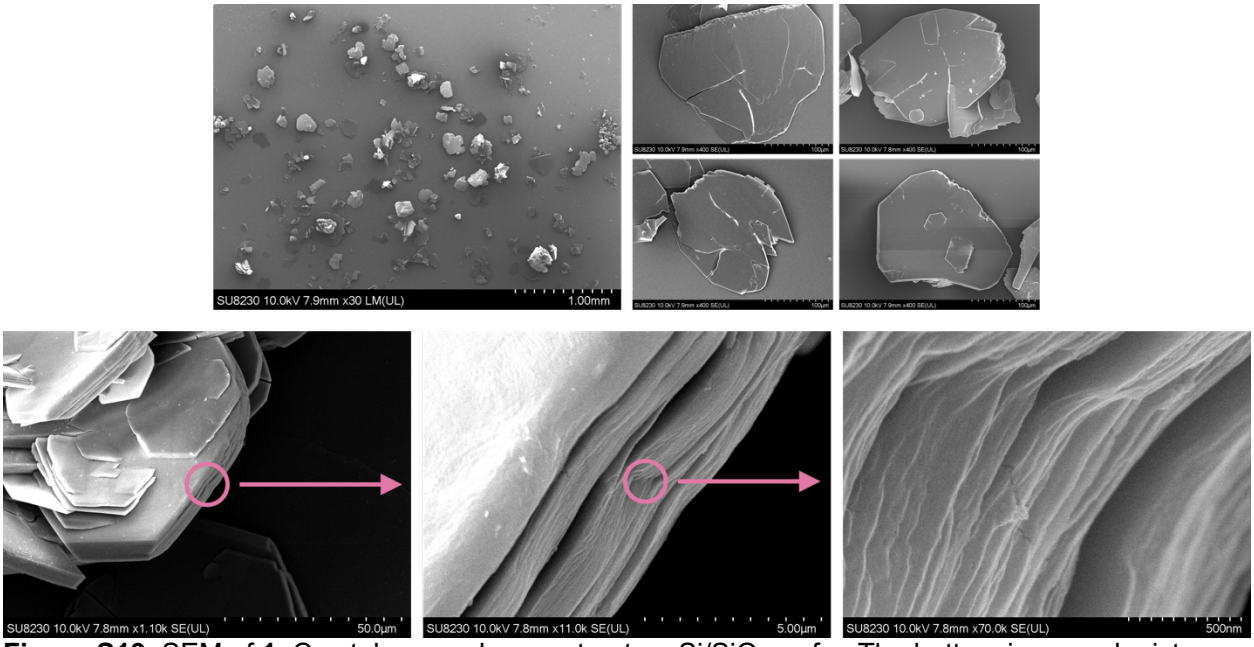

Figure S13. SEM of **1**. Crystals were drop cast onto a Si/SiO_2 wafer. The bottom images depict same flake, with the circled portion indicating the magnified area in the adjacent image.

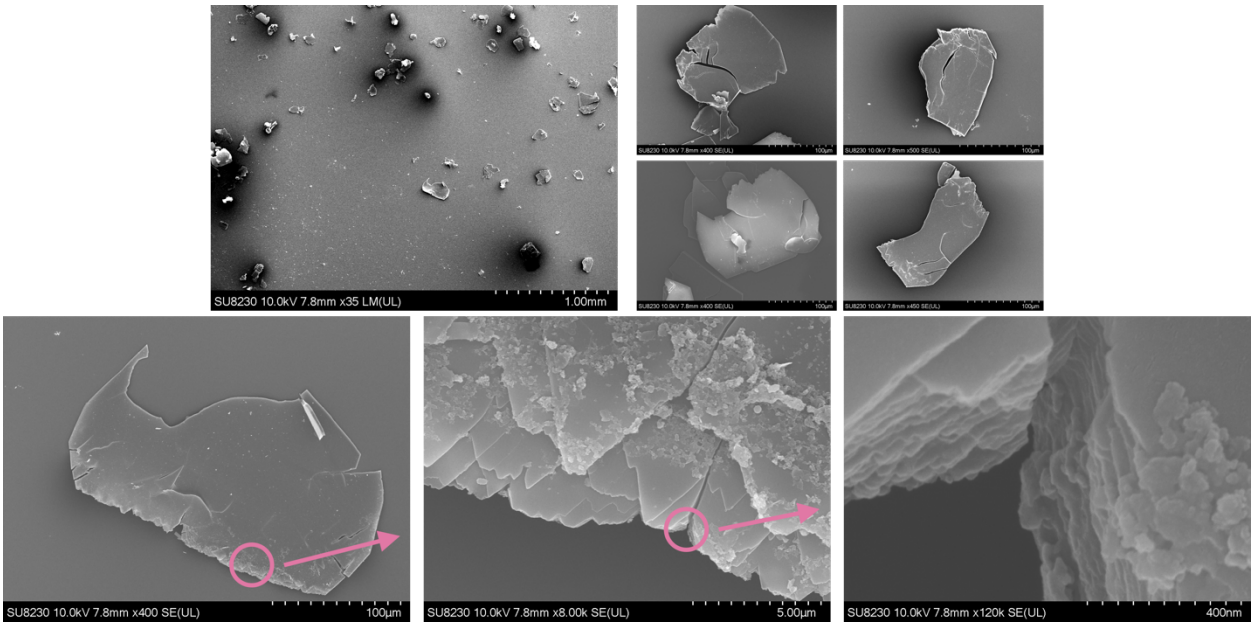

Figure S14. SEM of **2**. Crystals were drop cast onto a Si/SiO_2 wafer. The bottom images depict same flake, with the circled portion indicating the magnified area in the adjacent image.

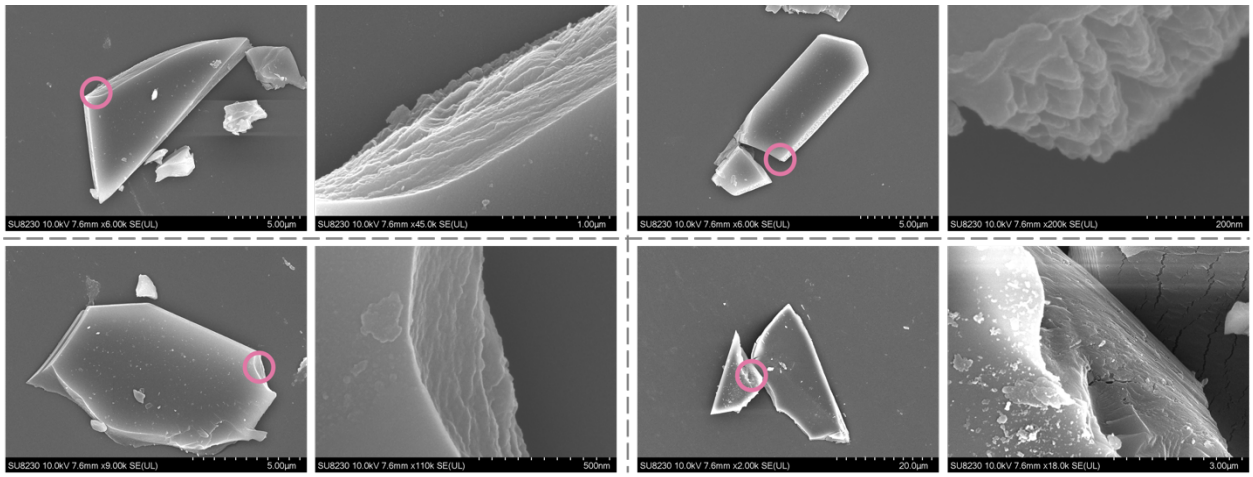

Figure S15. SEM of **2** exfoliated onto a Si/SiO_2 wafer. The image pairs depict same flake, with the circled portion indicating the magnified area in the adjacent image.

H. X-Ray Photoelectron Spectroscopy

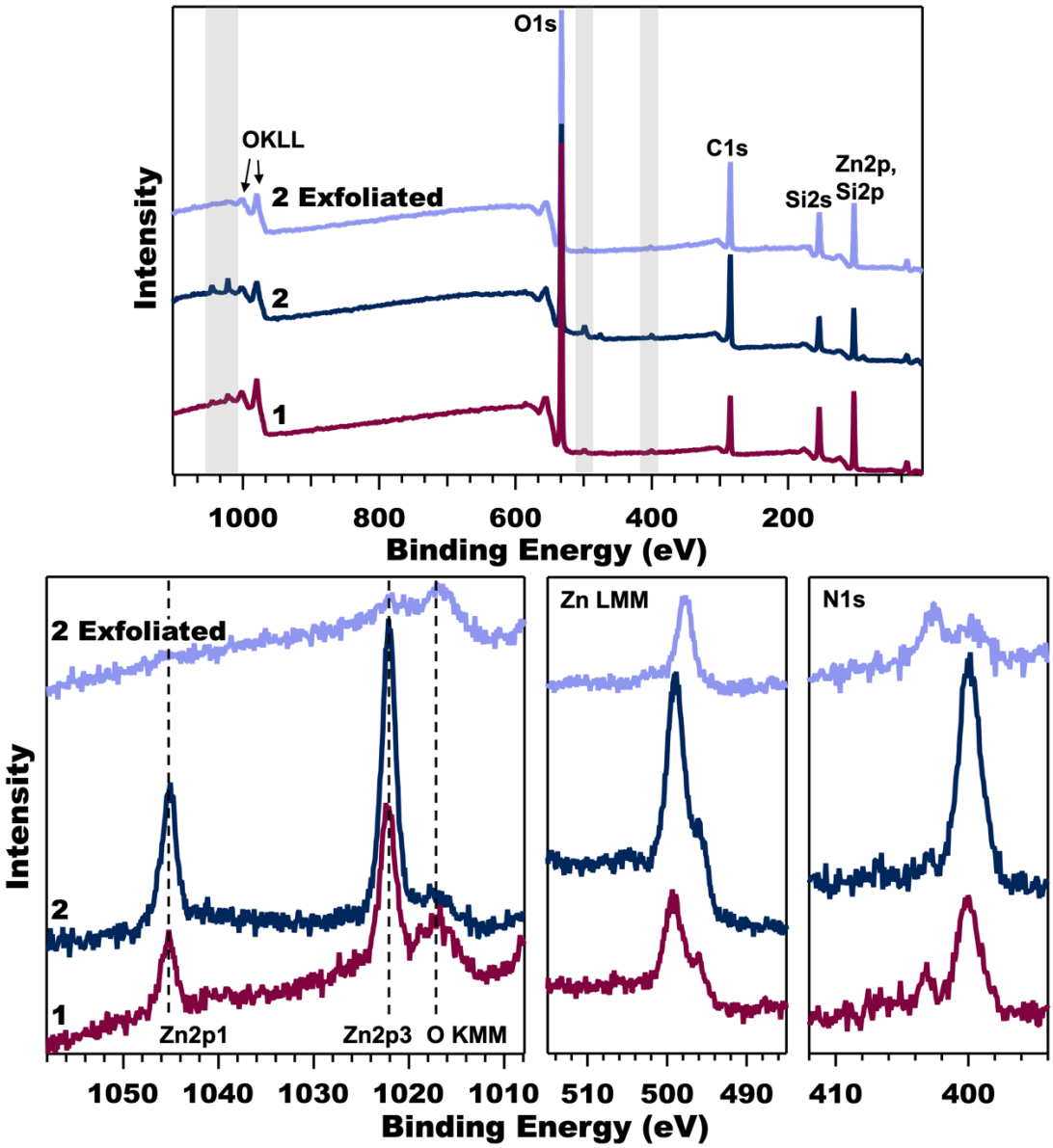

Figure S16. Full XPS spectra of **1**, **2**, and exfoliated MOF **2** (top). Shaded areas are expanded on in the bottom plots. Peaks were labelled according to literature values of binding energies.[13]

I. Atomic Force Microscopy

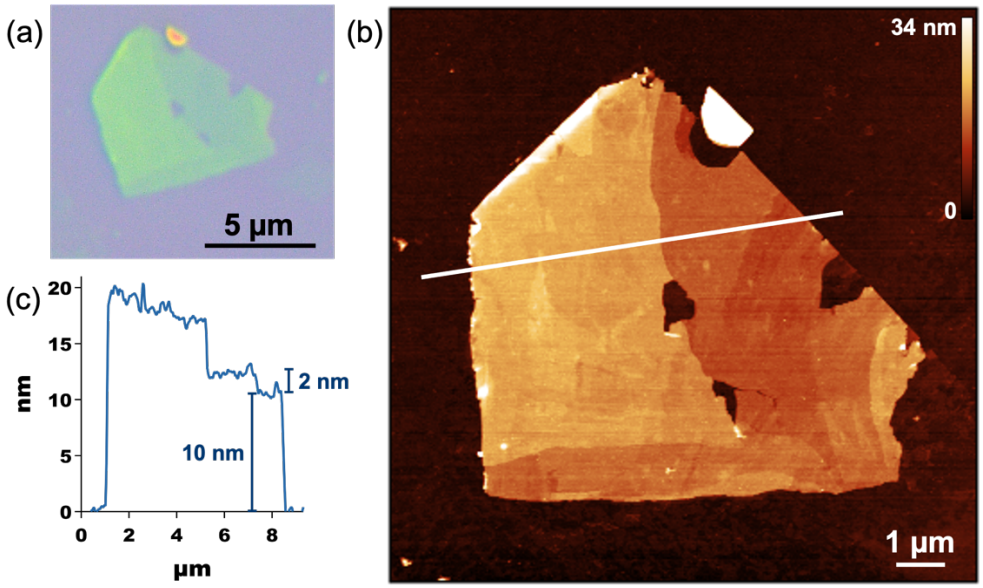

Figure S17. Optical image (a) of an exfoliated flake of **2** on a Si/SiO_2 wafer, their AFM topography map (b), and height profiles (c).

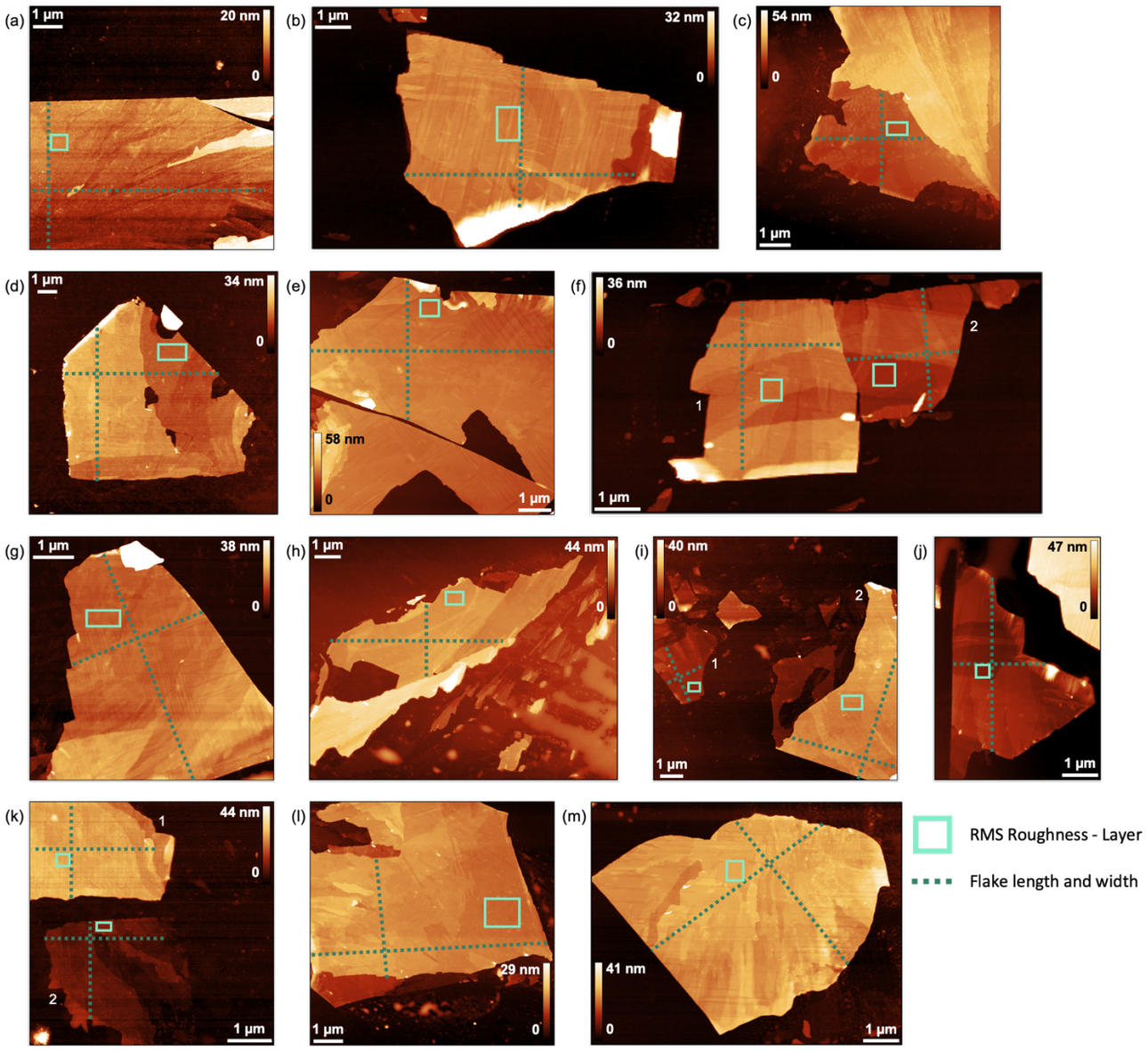

Figure S18. AFM topography map of exfoliated flakes of **2**. A solid box outlines the area sampled for root mean square (RMS) roughness. Dotted lines represent the length and height used to estimate the flake's area as a rectangle.

Table S1. Measurements of exfoliated flakes of **2**. The approximated aspect ratios (area: thickness) of the sampled flakes, determined by AFM, range from 274 nm to 4697 nm, with an average of 1560 nm (σ = 1190 nm). Although exfoliated flakes ranged largely in sizes, their large positive aspect ratios validate the exfoliation ability of this 2D MOF.

Flake	RMS Roughness - layer (nm)	RMS Roughness - flake (nm)	Estimated Area (nm^2)	Average Thickness (nm)	Aspect Ratio[a] (nm)
a	0.684	2.73	4.13E+04	8.8	4.70E+03
b	0.464	1.73	2.20E+04	15.9	1.38E+03
c	0.362	2.08	1.23E+04	11.9	1.04E+03
d	0.563	3.77	6.11E+04	15.5	3.94E+03
e	0.590	3.40	3.35E+04	23.3	1.44E+03
f1	0.286	2.24	1.08E+04	15.8	6.81E+02
f2	0.179	2.03	6.34E+03	11.7	5.42E+02
g	0.505	2.52	1.96E+04	15.6	1.26E+03
h	0.416	1.50	1.94E+04	14.4	1.35E+03
i1	0.399	1.58	5.13E+03	9.24	5.56E+02
i2	0.604	1.94	3.18E+04	18.7	1.70E+03
j	0.391	2.44	1.21E+04	13.0	9.33E+02
k1	0.737	2.24	6.44E+03	23.5	2.74E+02
k2	0.782	2.17	6.48E+03	3.8	1.70E+03
l	0.366	1.59	3.50E+04	15.7	2.23E+03
m	0.212	2.10	2.88E+04	22.7	1.27E+03
Average	0.471	2.25	2.20E+04	15.0	1.56E+03
Standard Deviation	0.179	0.63	1.57E+04	5.4	1.19E+03

[a]Aspect ratio = estimated area/average thickness

J. Pictures of Pristine and Annealed Crystals

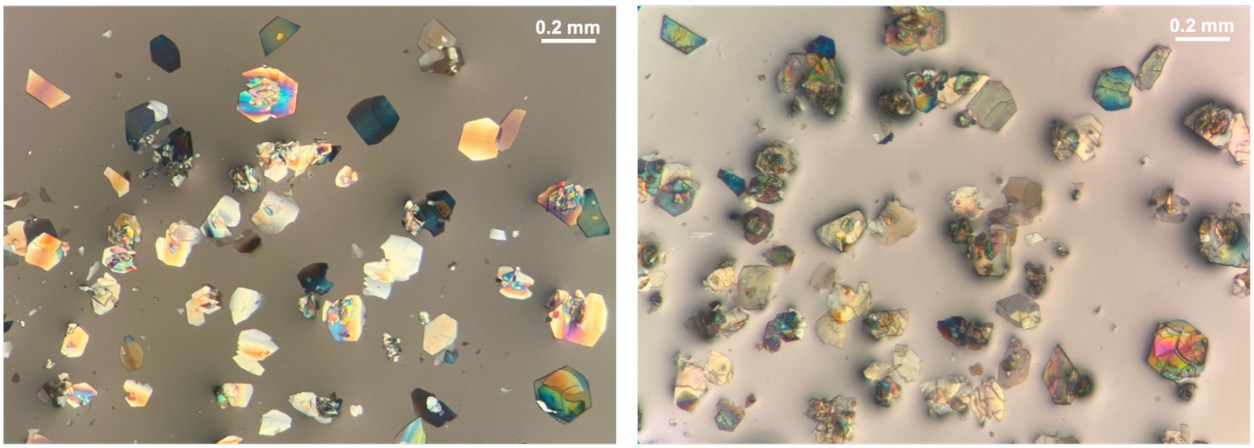

Figure S19. Optical images of crystals of pristine **1** (left) and **2** (right) annealed at 210°C for 10 min.

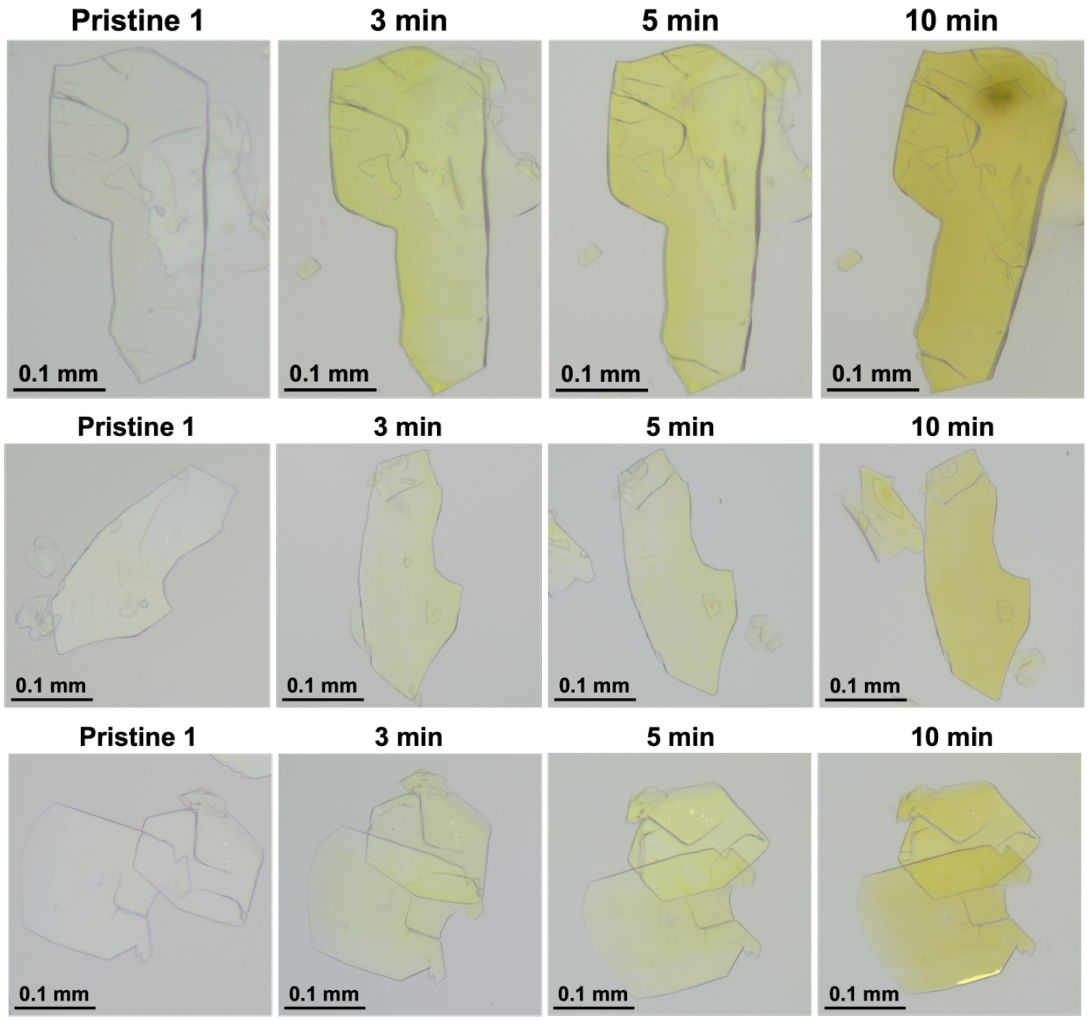

Figure S20. Optical images tracking single crystals of **1** throughout the annealing process with an annealing temperature of 210 °C.

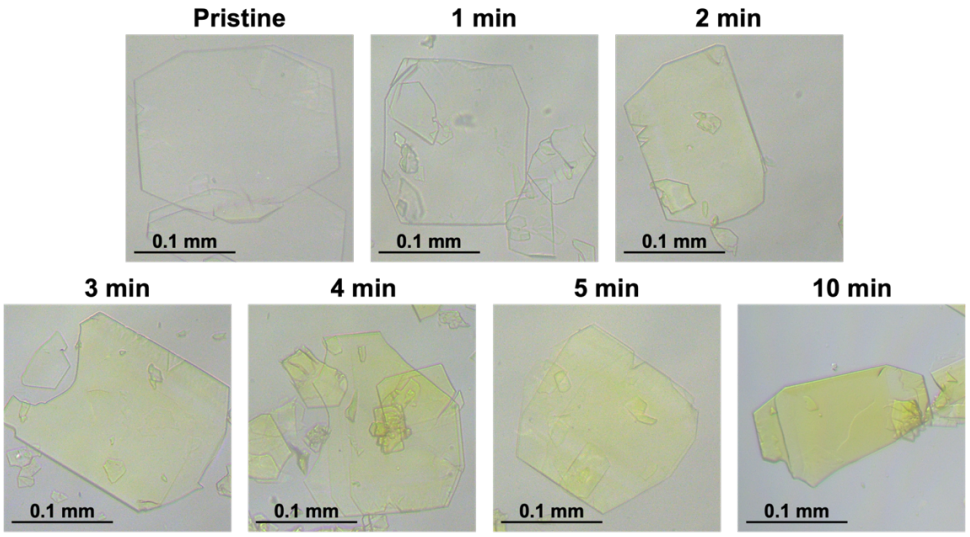

Figure S21. Optical images of pristine and annealed crystals of **1** with an annealing temperature of 210 °C over the course of 10 minutes.

K. Exfoliation Techniques

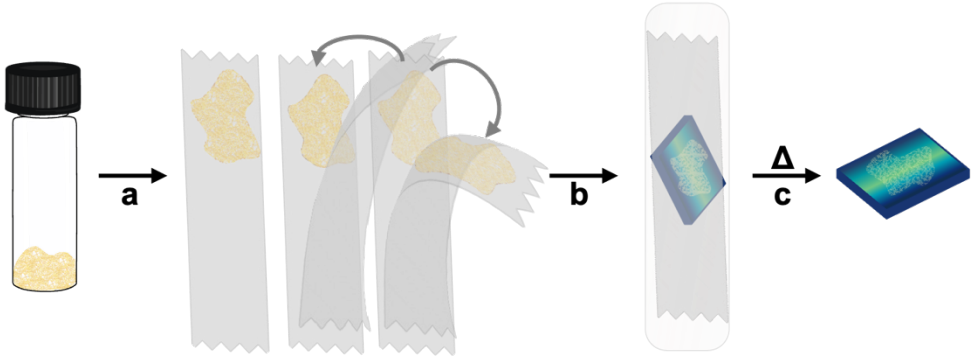

Figure S22. The general Scotch tape exfoliation process. Crystals of **2** are placed on the sticky side of a piece of Scotch tape (a). Another piece of tape is placed on top and pulled off. The tape is then placed on a plasma etched Si/SiO2 wafer on a glass slide (b). After annealing at 100 °C, the tape is pulled off the chip, leaving a layer of exfoliated flakes (c).

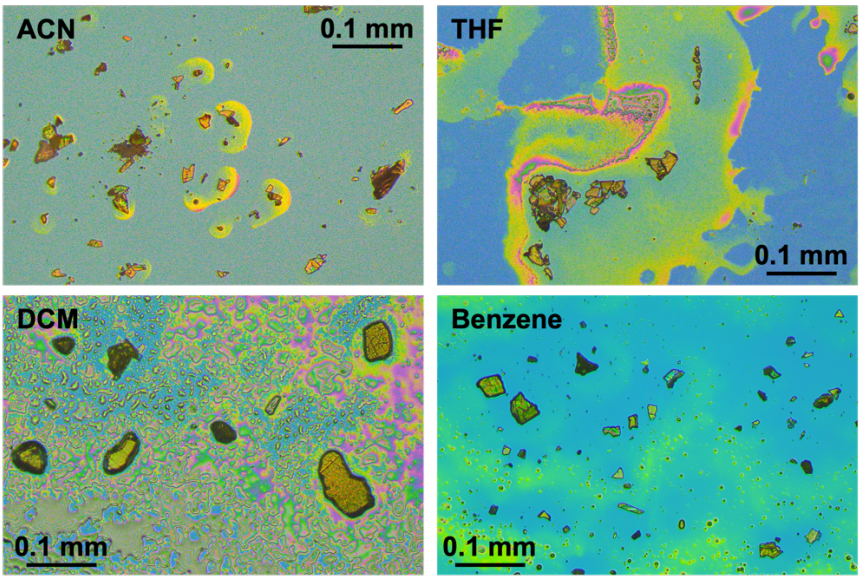

Figure S23. Exfoliation attempts by sonicating **2** in acetonitrile (ACN), THF, dichloromethane (DCM), and benzene. Crystals of **1** were annealed for 18 h at 160 °C and were sonicated for 9 h. Crystals were drop cast onto a Si/SiO_2 wafer. All attempts at exfoliation through sonication produced thick, small chunks of crystals along with residue left from solvent.

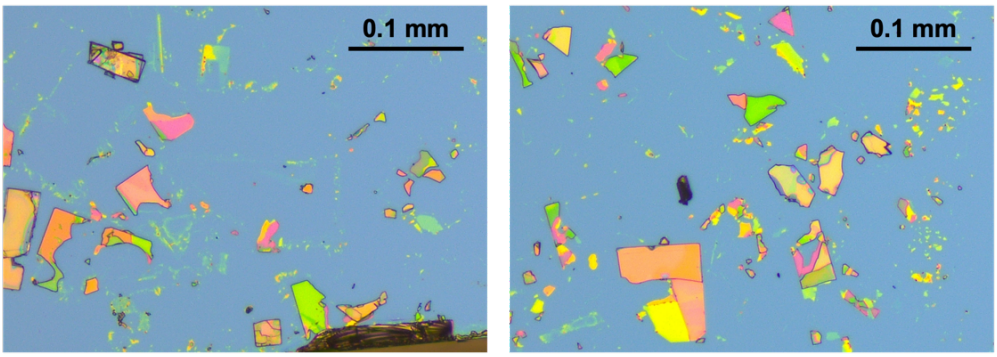

Figure S24. Optical images of **$Zn_3(BDC)_3(Py)_2$** exfoliated by the Scotch tape method onto a Si/SiO_2 wafer.

L. X-Ray and Electron Diffraction and Refinements

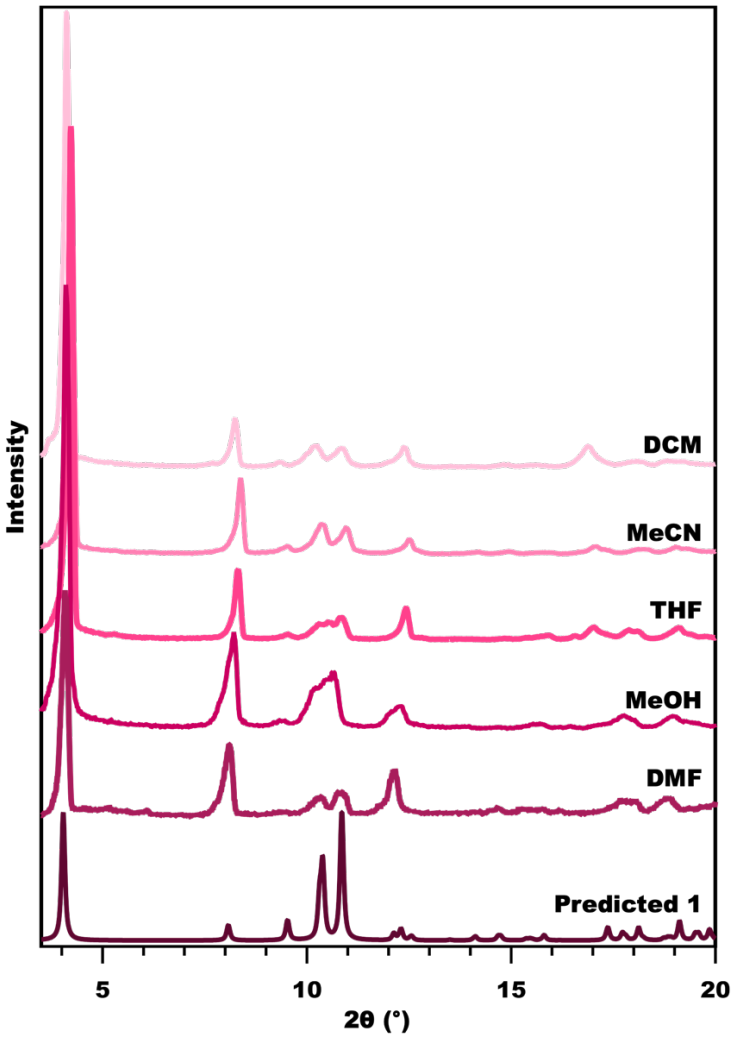

Figure S25. Powder XRD of pristine crystals of **1** after soaking in various solvents for 24 h.

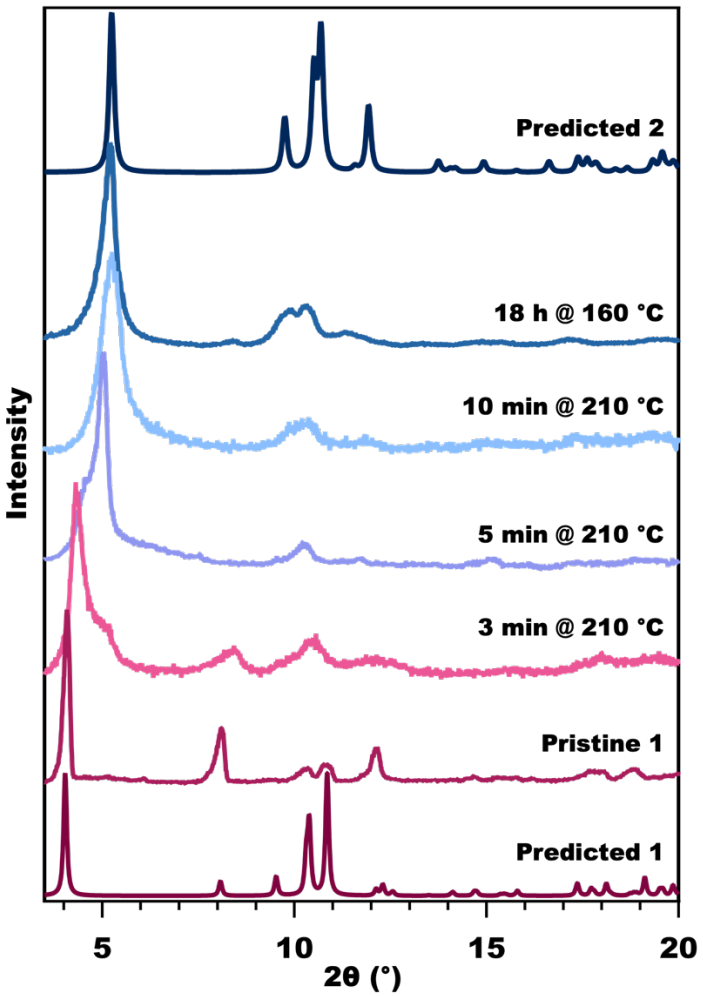

Figure S26. Powder XRD of pristine crystals of **1**, annealed crystals, including under exfoliation conditions (18 h @ 160 °C), and calculated spectra from the XRD and MicroED structures of **1** and **2**, respectively.

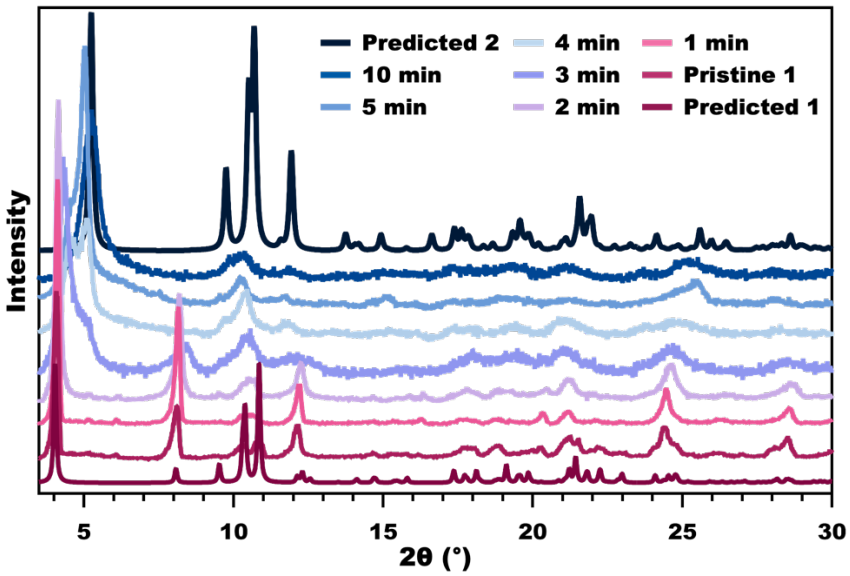

Figure S27. Full powder XRD of pristine crystals of **1**, crystals annealed at 210 °C, and calculated spectra from the XRD and MicroED structures of **1** and **2**, respectively.

$Zn_3(BDC)_3(diAn^{CNC\text{-}3Py})$ (1). The structure was solved in the monoclinic space group $P2_1/C$ with four molecules of DMF per unit cell. The asymmetric unit was found to contain two full molecules of DMF. There was no solvent disorder or positional disorder in **1**.

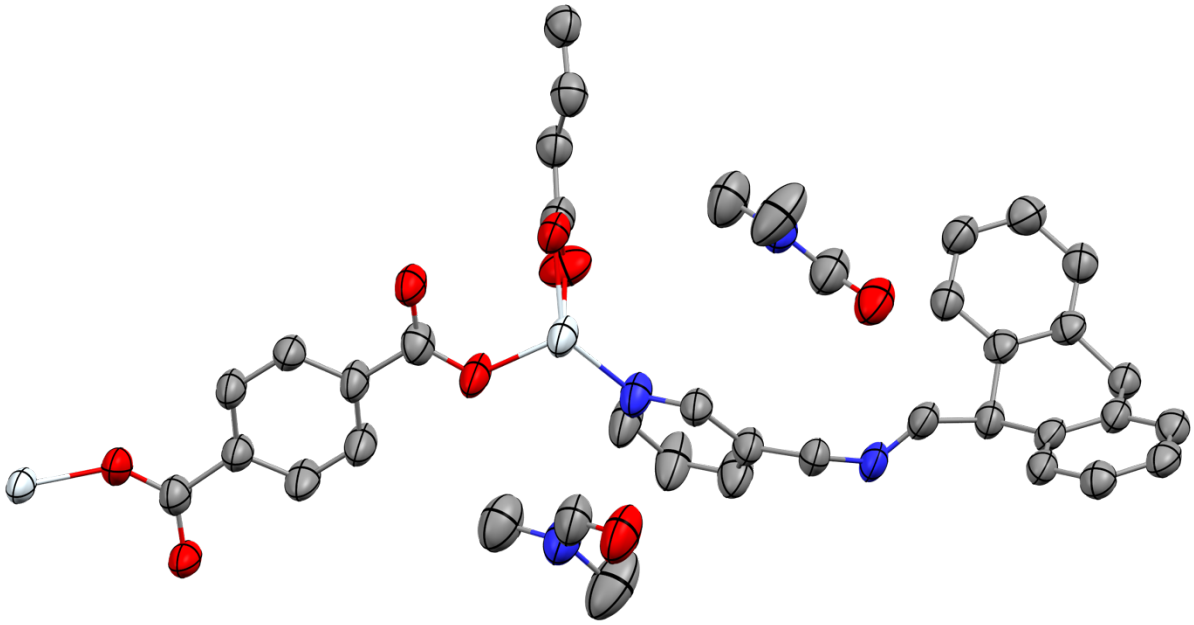

Figure S28. Asymmetric unit of **1** with thermal ellipsoids at 50% probability. Hydrogen atoms omitted for clarity. Color scheme: Zn, white; O, red; N, blue; C, gray.

$Zn_3(BDC)_3(An^{CNC\text{-}3Py})_2$ (2). Single crystals of **1** were annealed at 210 °C for 3 minutes. Data collected from 3 crystals were used to refine the model associated with this CIF on a XtaLAB Synergy-ED, HyPix-ED, electron source at 200 keV diffractometer. The structure was solved in the monoclinic space group $P2_1/C$.

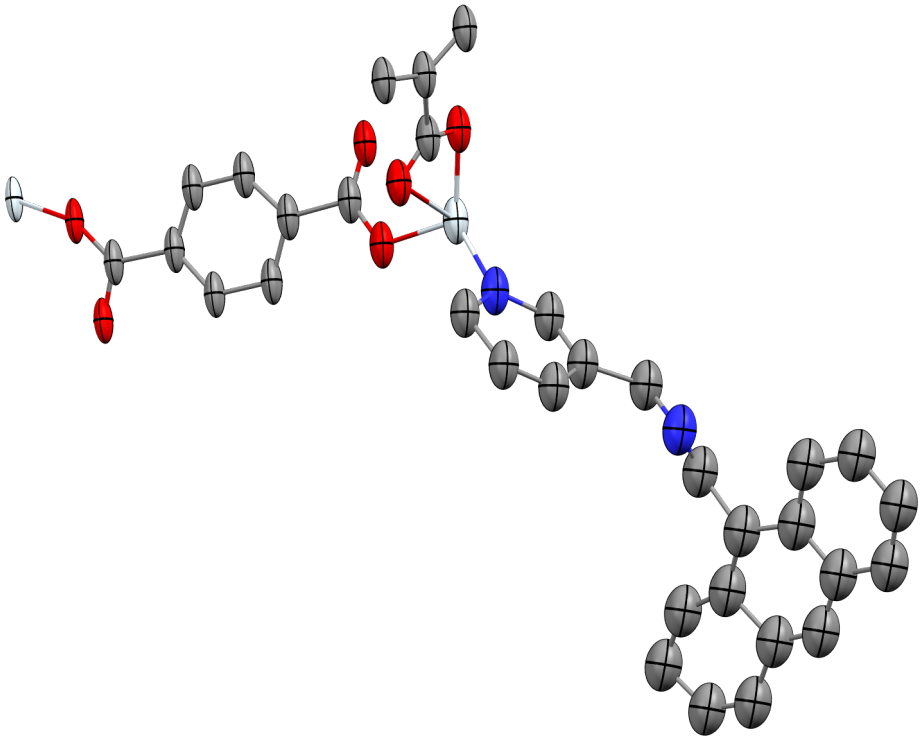

Figure S29. Asymmetric unit of **2** with thermal ellipsoids at 50% probability. Hydrogen atoms omitted for clarity. Color scheme: Zn, white; O, red; N, blue; C, gray.

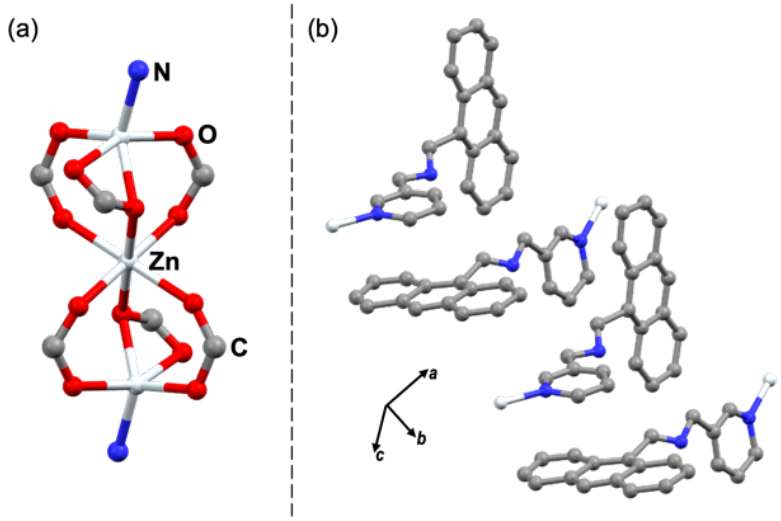

Figure S30. Metal node of **2** (a) and the stacking of $An^{CNC\text{-}3Py}$ within the lattice of **2** (b) with the metal node reduced to a single zinc atom and hydrogen atoms omitted for clarity.

Table S2. Crystallographic data for $Zn_3(BDC)_3(diAn^{CNC\text{-}3Py})$ (**1**) and $Zn_3(BDC)_3(An^{CNC\text{-}3Py})_2$ (**2**).

	1	**2**
Chemical formula	$C_{78}H_{72}N_8O_{16}Zn_3$	$C_{66}H_{44}N_4O_{12}Zn_3$
Formula weight	1573.54	1281.26
Space group	$P2_1/c$	$P2_1/c$
***a* (Å)**	23.3813(11)	16.9(5)
***b* (Å)**	8.8522(4)	9.5(2)
***c* (Å)**	18.8122(9)	18.2(3)
α (deg)	90	90
β (deg)	111.915(5)	94.7(3)
γ (deg)	90	90
***V* (Å^3)**	3612.3(3)	2910(118)
Z	2	2
μ (mm^{-1})	1.782	0.000
T (K)	100.00	100.00
GOF (S) [all data]	1.030	1.011
***R*1[a] (*wR*2[b]) [*I*>2σ(*I*)]**	0.0788 (0.1936)	0.2263 (0.5061)
***R*1[a] (*wR*2[b]) [all data]**	0.1297 (0.2230)	0.2839 (0.5386)
Reflections	6548	13047
Radiation type	Cu *K*α	electron (λ = 0.0251)

[a]$R1 = \Sigma[w(F_o - F_c)]/\Sigma[wF_o]$; [b]$wR2 = [\Sigma[w(F_o^2 - F_c^2)^2]/\Sigma[w(F_o^2)^2]]^{1/2}$, $w = 1/[\sigma^2(F_o^2) + (aP)^2 + bP]$, where $P = [\max(F_o^2,0) + 2(F_c^2)]/3$

M. References

1. O. V. Dolomanov, L. J. Bourhis, R. J. Gildea, J. A. K. Howard and H. Puschmann, *J. Appl. Cryst.*, 2009, **42**, 339-341.
2. G. M. Sheldrick, *Acta Cryst.*, 2015, **A71**, 3-8.
3. G. M. Sheldrick, *Acta Cryst.*, 2015, **C71**, 3-8.
4. S. A. Zarei, K. Akhtari, M. Piltan, S. M. Kamel and J. T. Mague, *Acta Cryst. C*, 2018, **74**, 480-486.
5. M. Ehrenberg, *Acta Cryst. B*, 1968, **24**, 1123-1125.
6. L. Yang, L. Qin, Y. Dou, D. Zhang, Z. Zhou and S. Wang, *CrystEngComm*, 2020, **22**, 5411-5415.
7. J. M. Masnovi and J. K. Kochi, *J. Am. Chem. Soc.*, 1985, **107**, 6781-6788.
8. G. Collet, T. Lathion, C. Besnard, C. Piguet and S. Petoud, *J. Am. Chem. Soc.*, 2018, **140**, 10820-10828.
9. S. Rojas, F. J. Carmona, E. Barea and C. R. Maldonado, *J. Inorg. Biochem.*, 2017, **166**, 87-93.
10. J. He, Y. Zhang, J. Yu, Q. Pan and R. Xu, *Mater. Res. Bull.*, 2006, **41**, 925-933.
11. S. S. 3-Picolylamine; CAS RN: 3731-52-0; A65409; Sigma Aldrich, St. Louis, MO, June 2023. https://www.sigmaaldrich.com/US/en/product/aldrich/a65409 (accessed July 16, 2024)
12. NIST Chemistry WebBook, SRD 69, Formamide, N,N-dimethyl, https://webbook.nist.gov/cgi/cbook.cgi?ID=C68122&Units=SI&Type=IR-SPEC&Index=2#IR-SPEC (accessed April 2, 2024).
13. J. F. Moulder, *Handbook of X-ray Photoelectron Spectroscopy*, Perkin-Elmer Corporation, 1992.